CAHIERS MAGELLANES-NS
Volume 06 Issue 2
2024

ISSN:1624-1940
DOI 10.6084/m9.figshare.2632574
http://magellanes.com/

ASSESSING CHANNEL MORPHOLOGICAL CHANGES AND CHANNEL MIGRATION OF RAMGANGA RIVER, INDIA USING REMOTE SENSING AND GIS TECHNIQUES

Rameswar Mukherjee[1] Pamela Deb [2]

1Assistant Professor,Dept.of Geography,Samsi College, Samsi,Malda,West Bengal,India

2Assistant Professor,Dept.of Geography, Amity University, Kolkata , West Bengal,India

Corresponding Author: Pamela Deb

Abstract

This study investigates the morphological changes and later movement of the Ramganga River from 1923–2014 based on remotely sensed data and topographic maps. It focused on the Rohilakhand Plain in the Western Gangetic Plain (WGP), India, where channel shift is common. This study utilized Landstat-MSS images from 1972–2014 and georeferenced the Topographical Sheet (NG 44–2) from the US Army Map Service, 1923. Various morphological parameters, such as channel width, sinuosity, braiding intensity, active channel area, and channel bar area, are used to monitor the lateral movement of the river. The result reveals the complex hydrodynamic mechanisms of the river, which include an increasing tendency for braiding, decrease in active channel width and length, increase in the number of cut-offs and channel avulsions, alternating eastward and westward migration, and alternating stages of increasing and decreasing sinuosity.

Key words: Channel morphology, Channel morphodynamics, Channel migration, Bankline migration, Western Gangetic Plain.

Introduction

Rivers are the restless creators of landscapes, continuously shifting valleys and flood plains under the strong currents bearing sediment loads. The form of river channels seeks a delicate equilibrium state, thereby balancing the erosive forces of streamflow against the resistance of the barrier materials creating by the bed and banks (Leopold et al. 1964; Lewin, 1977; Knighton, 1984). In this equilibrium condition, the energy consumption of the river is optimized, and efficient flow free from noteworthy morphological change is possible. But this dynamic equilibrium is easily disturbed. Changes in independent factors such as discharge, sediment supply, or the erosive resistance of border materials might throw off the balanced condition (Schumm, 1977; Morisawa, 1985). Natural phenomena like fluctuations in climate could cause such changes in sediment flow from the drainage basin. But the triggers upsetting this delicate equilibrium in river channels are increasingly human activities including land use changes, water resource development projects, and instream channel modifications.

When this equilibrium is disturbed by a set of actions aimed to either release extra energy or match new hydrologic and sediment regimes, rivers respond. This channel instability starts a sequence of morphological changes involving width, depth, slope, sinuosity, and erosion/deposition patterns as the river discovers a new quasi-equilibrium form. The modifications are achieved in part by erosional and depositional processes reworking boundary materials, distributing silt, and altering the river's route across its floodplain over time (Robert,2014, Mukherjee, 2022).

Knighton (1984) explained four main components which can help to evaluate the dynamics of channel

ISSN:1624-1940
DOI 10.6084/m9.figshare.2632574
http://magellanes.com/

form produced by internal geometry transformations:

i. **Cross-sectional form**: This element describes a river's cross-sectional shape, size, and layout at any one location or reach. It displays the river's material flow capacity as well as the erosional, or depositional, processes taking place at that location.

ii. **Channel bed form**: It represent structure of the channel beds, mostly made of sand and gravel. It shows the several forms or features moulded out of the channel bed by large deposits like Riffles, pools, and bars, these components show the dynamics of river force and sediment transport.

iii. **Planform geometry**: From an overhead perspective, it reveals a two-dimensional channel configuration. Typically following their planforms, channel patterns are either braided, straight, or meandering. River slope, outflow, and sediment load affect planform geometry.

iv. **Channel bed slope**: It depicts the gradient of the channel bed along a certain stream reach. While localized slopes change, the longitudinal profile, which takes into account the entire reach, provides a more complete picture of the river's energy dissipation and sediment transport capacities.

However, the knowledge about channel morphology is necessary to understand the intricate mechanisms of river systems and their response to environmental conditions. Understanding the past of the river helps one to predict future changes in river systems and to know the pattern of channel morphodynamics (Winterbottom, 2000). From a historical viewpoint, aerial photographs and satellite image enable one to examine contemporary fluvial processes and channel structural change (Petts, 1989; Trimble and Cooke, 1991; Gurnell, 1994, 1997). Most of the visual depiction on channel morphodynamics are provided by these data sources. Usually, though, their availability covers just the past 60 years. Although some topographic maps, survey maps, and charts have existed for more than 300 years in some parts of the world, these resources are often available at wide intervals—mostly more than 50 years, which makes it difficult to attribute sequential changes in morphodynamics on a decadal or annual basis.

As human pressures on river environments become more severe, developing quantitative knowledge of channel dynamics with the help of multi-temporal aerial photographs and satellite images and integrating with GIS becomes vital for sustainable river management and restoration initiatives. This study attempted to understand the morphological changes and lateral migration pattern of Ramganga river based on remotely sensed data and topographic maps for 91 years.

Review of literature

Channel Migration

Channel migration patterns and rates have been the subject of extensive research. Hickin and Nanson (1975) discussed the patterns of channel migration, calculated migration rates, and deciphered the role of channel avulsion in determining the dynamics of channel migration. Goswami et al. (1999) studied the sequential changes in the position of the Subansiri River channel between 1920 and 1990 in Assam, India. Lane et al. (2003) generated Digital Elevation Models (DEMs) for calculating the rates of erosion and deposition as well as channel changes using digital photogrammetry, laser altimetry, and image processing techniques. Richard et al. (2005) measured the lateral channel migration rates using statistical methods of Rio Grande River. The found that the degree of braiding and flow energy both influence the lateral channel migration. Baldwin et al. (2006) demarcated paleochannels using satellite images, borehole data, and high-resolution seismic-reflection data to assess Pee Dee River flow trends

ISSN:1624-1940
DOI 10.6084/m9.figshare.2632574
http://magellanes.com/

in the USA. Jian et al. (2009) tracked the spatio-temporal characteristics of channel changes in the Yangtze River in order to assess how both natural and anthropogenic factors affected these fluctuations. Phillip (2009) elucidated the methods and evolution of avulsion as well as the controlling variables by combining aerial photos, DEMs, and field survey data. Zawiejska and Wyzga (2010) investigated the geographical and chronological trends of channel migration of the Dunajec River using historical maps, hand-auger drillings in paleochannels, and hydrometric data from gauging stations.

Bank erosion and bank line Migration

River bank erosion and accretion have been of long-standing interest among engineers and Earth scientists. Researchers have studied these processes over various intervals to understand their dynamics and rates (Wolman, 1959; Twidale, 1964; Knighton, 1973). As technology advanced, new methods emerged for observing and quantifying these processes. Topographical maps and aerial imagery have allowed researchers to identify and analyze trends in bank erosion and accretion over larger spatial and temporal scales (Lewin, 1972; Hickin & Nanson, 1975; Hooke, 1980; Lawler et al., 1997).

With the advent of satellite data and Geographic Information Systems (GIS), extensive spatio-temporal monitoring of bank erosion and accretion processes has become progressively possible. Winterbottom and Gilvear (2000) analyzed the river bank erosion in the controlled River Tummel, Scotland, by using a GIS-based probabilistic approach. Bartley et al. (2008) forecasted bank line erosion in tropical catchments using erosion pins, benchmarked cross-sections, and previous aerial images. Likewise, with a Hydrographic Atlas and SPOT 5 satellite images, Kummu et al. (2008) approximated the rates of bank erosion and accretion for the Mekong River. Yao et al. (2011) looked at Yellow River bank erosion and accretion using GIS using maps created from field research, aerial photographs, and satellite imagery. Baki and Gan (2012) evaluated the trend and rates of bank erosion and accretion of the braided Jamuna River using Landsat data from 1973–2003, therefore raising knowledge of the effect of different discharge and river widths on erosion and accretion processes. Aside from conventional methods, researchers have employed various methodologies to assess river bank erosion. Thoma (2001) used laser altimetry, whereas Jia et al. (2010) developed a 3D model to simulate river bank erosion over the middle Yangtze River. Grove et al. (2013) utilized multi-temporal LiDAR and high-resolution aerial imagery to assess the degree and causes of bank erosion after severe floods. Nardi et al. (2013) used shear stress models and hydrodynamic models (1D and 2D) to monitor bank erosion in the River Cecina in Tuscany.

Furthermore, the studies by Indian scientists are very helpful for investigating bank erosion and accretion. Bhakal (2005) looked at bank erosion along the Brahmaputra River using GIS. In 2005, Kotoky et al. examined rates of migration along the Brahmaputra River and bank line erosion process in Assam, India. Sharma and Goswami (2007) explored the sequential bank line migration brought on by bank erosion and accretion of the Burhi Dihing River (Assam) using Survey of India Toposheets and satellite data. In 2012, Sinha and Ghosh examined the Ganga River's channel morphology and bank erosion across time. The Subansiri and Ranganadi rivers' bankline erosion in Northeast India was reported by Das et al. (2012). Bandyopadhyay et al. (2014) put up an RS-GIS-based model for identifying bank erosion sensitivity zone along the Haora River Tripura, India. Bhowmik and Das (2014) identified sites probably experiencing bank erosion using GIS overlay analysis. Thakur (2014) assessed bank erosion in the Ganga River upstream from the Farakka Barrage to Rajmahal using

ISSN:1624-1940
DOI 10.6084/m9.figshare.2632574
http://magellanes.com/

LANDSAT and IRS satellite image. Mukherjee et al. (2017) carefully examined bank erosion and accretion dynamics of the Ramganga River using multi-temporal topographical maps and satellite images, so clarifying the expected mechanisms of bank erosion and accretion over the selected study reach.

Channel morphodynamics

Using remote sensing, GIS, field surveys, and statistical analysis researchers have examined the dynamics of channel morphology (e.g. Bertoldi et al., 2009; Yang et al., 2013; Midha and Mathur, 2014; Sinha et al., 2014; Arnaud et al., 2015; Clerici et al., 2015; Nawfee et al., 2018; Roy and Sinha, 2018; Akhter et al., 2019; Pal and Pani, 2019; Agnihotri et al., 2020; Kong et al., 2020; Majumdar and Mandal, 2020; Mahmud et al., 2020 Rashid, 2020; Rashid et al., 2021; Khan et al., 2022; Mukherjee, 2022). These techniques have made it easy to estimate channel morphometric parameters, evaluate spatiotemporal variations, and find the fundamental causes of planform changes. Dramatic channel morphological changes in many modern channels have been brought about by artificial disturbances including land-use changes (Karwan et al. 2001; Ghimire and Higaki, 2015; Williams and Wolman, 1984; Surian, 1999; Grant et al., 2003; Vörösmarty, 2003; Yang et al., 2015) as well as climate change (Ashmore and Church, 2001; Feng, 2011; Chang, 2008; Kiss and Blanka, 2012) and sand and gravel mining (Wishart et al., 2008).

Channel morphodynamic and channel migration studies are the quantification of channel morphological characteristics and evaluation of their spatio-temporal variations. Various studies have also concentrated on the factors influencing elements in planform dynamics (Anderson and Calver, 1980; Hooke and Redmond, 1992). Strong causal elements for channel morphological change and migration in a short period are considered to be variations in discharge and stream power (Lewin, 1983; Hickin and Nanson, 1984).

Study Area

The Ramganga River is one the major tributaries of the Ganga River, which joins the Ganga near Kannauj, Uttar Pradesh, India. The Ramganga River has a 30,635.1 km² watershed area. Beginning in the Lesser Himalaya at 2,926 m ASL close to Gairsen, Chamoli District, Uttarakhand, it comes from the Dudhatoli Crystalline Formation (Mukherjee et al., 2017). The river runs roughly 649.11km overall, with 481.2 km on the Western Gangetic Plain and 167.91 km across the Himalayan area.

The present study focuses especially on the area known by the local population as the Rohilkhand Plain (Fig. 1) in the Western Gangetic Plain (WGP). The regular channel shift of this part of the river is a common phenomenon in this region. The morphological features like numerous meander scars, swale, and ridge series, and many abandoned channels, chute channels, and paleochannels validate this fact which further suggests that the river bends are horizontally instable (Mukherjee and Deb, 2024).

Here the Ramganga River exhibits both partly braided and single-thread meandering channel pattern. The river gradient is far higher than in the main Eastern Gangetic Plain rivers which causes to produce a higher stream power.

Köppen's climatic classification places designates this region as Cwg climate type. Dry winters define this sort of climate. With an average annual rainfall of between 160 and 180 cm, the monsoon season,

CAHIERS MAGELLANES-NS
Volume 06 Issue 2
2024

ISSN:1624-1940
DOI 10.6084/m9.figshare.2632574
http://magellanes.com/

which runs from June to September, explains almost 80 percent of the total annual rainfall. The temperatures in summer can rise beyond 40°C, and in winter, they might drop below 10°C (Mukherjee, 2022).

Geologically Rohilakhand Plain has three primary layers: Varanasi older alluvium, Ramganga terrace alluvium, and Ramganga recent alluvium (Khan and Rawat, 1992; Mukherjee et al. 2017). Beside the current path of the Ramganga River lies the recent alluvium formed by the sediments carried by the river. The regular floods cause major changes in this unit. Ramganga terrace alluvium is located well above the current channel floor (>6 m), submerged only during rare mega-flood events, it is linked to historic floodplains and elevated terrace surfaces (Mukherjee et al., 2017). The great richness of clayey-silt soils and the presence of calcium-rich "*kankar*" (calcareous nodules) set this unit apart. The Varanasi older alluvium is found on raised terrace surfaces and sandy alluvial ridges Commonly known as "*Bhur*". Former routes of the Ramganga River produce the *Bhur* ridges (Shrivastava et al., 2000).

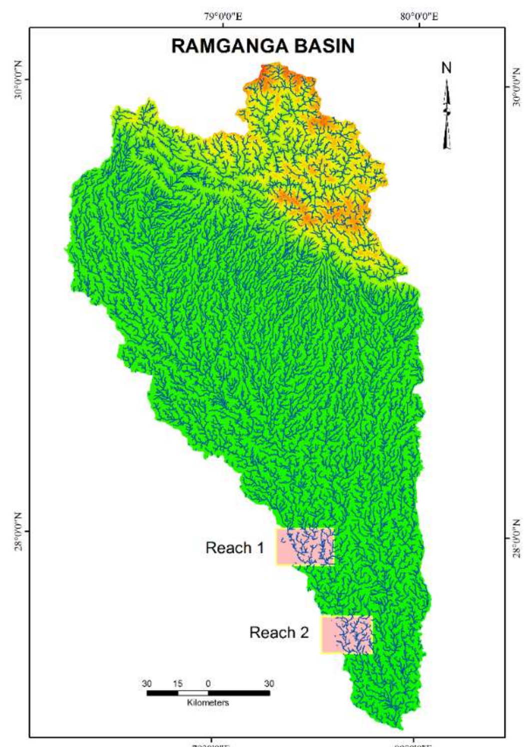

Fig. 1

The monsoon is the key driver of the Ramganga River's hydrological regime, introduces distinct seasonal variations in discharge, silt load, and stream power. Usually running from June to September, the monsoon season provides a lot of precipitation to the Ramganga watershed, so influencing rather high river flow rates. During this period, the river experiences a significant surge in flow rates, often leading to overbank flooding and the inundation of adjacent floodplains. This high-energy flow regime, facilitates the erosion and transit of sediments through lateral migration, avulsion, and the formation of new depositional features, thereby reshaping the channel geometry.

Moreover, the greater silt load the Ramganga River carries during the monsoon greatly affects channel dynamics. The channel bed's greater sediment load may lead to aggrade, therefore altering the river's

ISSN:1624-1940
DOI 10.6084/m9.figshare.2632574
http://magellanes.com/

slope and promoting the growth of braided or anabranching patterns. Conversely, times of heavy discharge mixed with inadequate sediment flow can lead to channel incision and the development of ever-shallow and narrow channels.

Data acquisition

Georeferenced and accurately orthorectified Landsat data downloaded from the Landsat look viewer website (Table 1). Landsat data were georeferenced with the following parameters-
Projection Type: Universal Transverse Mercator (UTM)
Spheroid Name: WGS 84
Datum Name: WGS 84
The study area belongs to UTM Zone 44. Three Landsat data scenes covering the whole study reach have been shown; the path row for 2014, 2003, and 1993 Images is 145 /41; for 1972 and 1981 images is 155 /41.

Image Processing

To preserve homogeneity in spatial resolution over all the satellite images used for this research, the Landsat-MSS images from 1972 and 1981 were rescaled into 30 meters using the resample tool in the ERDAS-IMAGINE 2014 application. The Topographical Sheet (NG 44-2) released by the US Army Map Service was georeferenced using the same parameters as Landsat satellite images.

Table 1: Data used in the study

Data type	**Satellite-sensor/Map No**	**Date (mm. dd. year)**	**Spatial resolution (m) or scale**	**Source**
Remote sensing Images	Landsat-MSS	2/19/1972	79	USGS
	Landsat-MSS	1/15/1981	79	USGS
	Landsat-TM	2/22/1993	30	USGS
	Landsat-ETM	2/27/2003	30	USGS
	Landsat 8-OLI	2/9/2014	30	USGS
Topographical Maps	NG 44-2	1922-1923 (surveyed) 1955 (Published)	1: 2,50,000	Series U502, US Army Map Service

Channel morphological Parameters

Overall, seven variables were used for characterizing the morphodynamics of the Ramganga River:

I. Active channel width
II. Channel sinuosity
III. Braiding index
IV. Active channel area
V. Channel belt area
VI. Active channel area

CAHIERS MAGELLANES-NS
Volume 06 Issue 2
2024

ISSN:1624-1940
DOI 10.6084/m9.figshare.2632574
http://magellanes.com/

VII. Channel belt area ratio
VIII. Sandbar area active channel area ratio

For showing lateral migration of the channel, two parameters have been considered:

I. Channel centreline migration and
II. Bank line migration

For determining the active channel width, the total extent of the wetted channel from a particular point was considered. For the images of the Landsat series, the MNDWI was applied to extract channel area by using the following formula:

MNDWI = (ρ Green – ρ SWIR)/ (ρ Green + ρ SWIR) (i)

Where ρ Green and ρ SWIR represent the reflectance of the green and shortwave infrared bands, respectively.

Then, the active channel width was measured through transects lying at an interval of 1 km. The sinuosity of the Ramganga channel was calculated in Arc GIS 10.1 by using the following equation:

CS= CL/VL (ii)

Where CS= channel sinuosity

CL= distance between two points along the channel centreline

VL= straight line distance between two points

The sinuosity of the channel was calculated by dividing the total channel length of the study reach to the straight-line distance of both the ends of the channel. To show the spatial variation of CS within the reach, equi-spaced section lines were drawn at an interval of 3 km.

The braiding index was calculated by using the formula of Brice (1964):

Braiding Index (BI) = (total length of the bar)/(length of the reach) (Brice, 1964) (iii)

By observing the nature and intensity of the braiding in the rivers of the Indo-Gangetic plain, the Braiding Index have been categorized into four sections to designate channel planform:

1 - 2 = Single thread
2 - 3 = Partly Braided
3 - 4 = Moderately Braided
> 4 = Intensely Braided

The Active Channel Area (ACA) was calculated from Landsat images by extracting water pixels using the MNDWI method. Following that, the pixels were transformed into polygons, and the ACA was calculated using Arc GIS's calculate geometry command. To demarcate the channel area in 1923, it was manually digitized from the topographical map. The channel belt area was digitally marked by measuring the amount of river channel dynamics within a valley. In this work, the channel belt was defined by tracing abandoned channels, meander scars, and paleochannel tracts.

The Centreline was drawn by connecting the midpoints of the active channel width that were 50 meters apart. After superimposing the subsequent years' centrelines, polygons were used to mark the lateral variation between them. After that, the area and perimeter of the polygons were determined using the following Micheli and Larsen (2011) formula:

Mean lateral change= Area/Half Perimeter (iv)

Delineation of Bank lines

ISSN:1624-1940
DOI 10.6084/m9.figshare.2632574
http://magellanes.com/

The frequent shifting of the Ramganga River made it impossible to define the bank lines. Although several automated bank line extraction algorithms are available, they need to produce consistent results for frequently migrating channels. The issue got more serious in the region where bank accretion predominated. Because the spectral reflectance of riverine tracts near the banks of these channels is very similar. As a result, identifying the banks required the expert's field knowledge. In the current study, manual digitization was carried out following many field observations. The work of digitizing bank lines from topographical maps became relatively simple because all of the banks were marked on the topo sheets.

Determining Bankline Migration

Thirty-seven transects were made at 500-meter intervals to map the migration of bank lines on a spatiotemporal scale. All transects were drawn parallel to one another. The shifting distance of the bank line was marked at each transect. The westernmost point of each transect was used as a reference point to determine bank line migration.

Result and Discussion

Lateral Migration of Channel

Channel Centreline Migration

In the reach 1, the maximum centreline migration was observed during 1972-1981, where the mean value was 43.28 m/year. It was followed by 1993-2203 (31.94 m/year), 1982-1993 (26.59 m/year) and 2003-2014 (25.66 m/year). Channel avulsion was common in all the periods. But the 1923-1972 and 1972-1981, channel avulsion was seen on a larger scale than any other periods (fig. 2).

In the reach 2, during 1923-1972, the whole channel shifted westward direction and the maximum value of MCM/year (40.67 m). All other periods also faced channel avulsion and local level cut-off. The maximum number of cut-offs was seen in 1993-2003 (12). It had a mean value of MCM/year 21.79 m and CV 0.83 (fig. 3).

CAHIERS MAGELLANES-NS
Volume 06 Issue 2
2024

ISSN:1624-1940
DOI 10.6084/m9.figshare.2632574
http://magellanes.com/

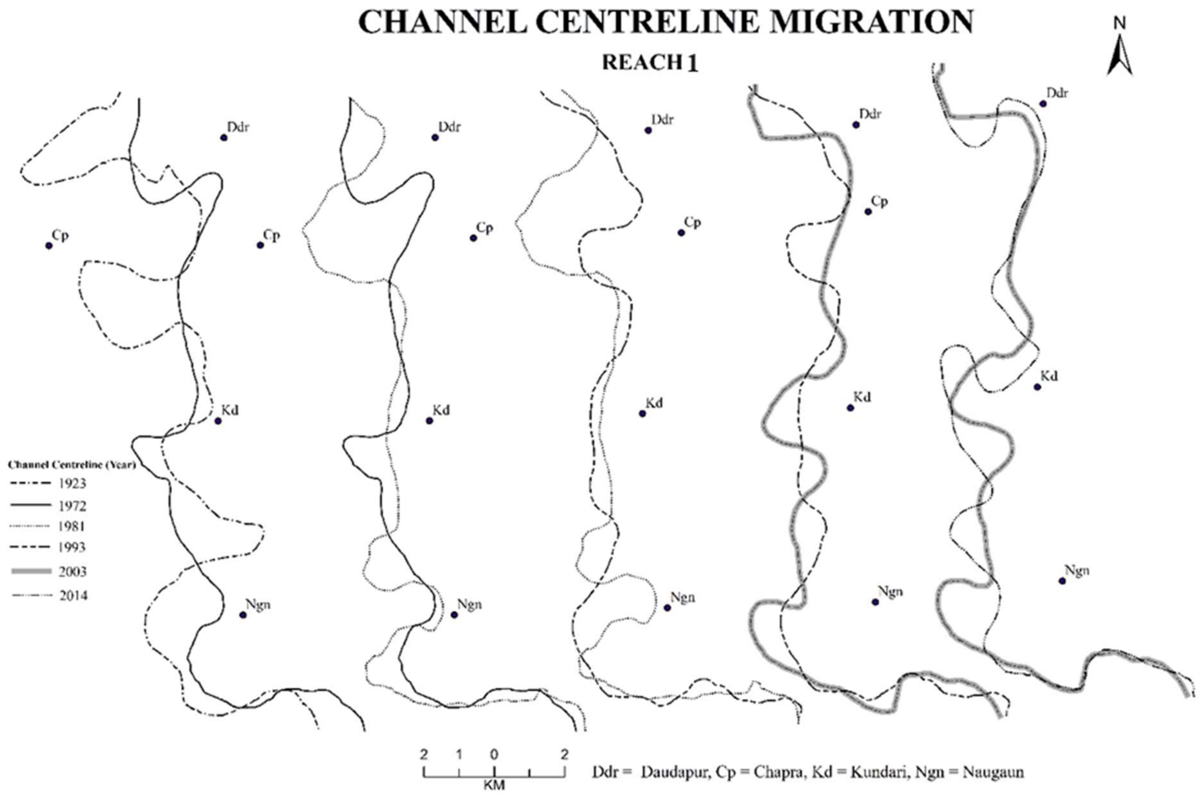

Fig. 2

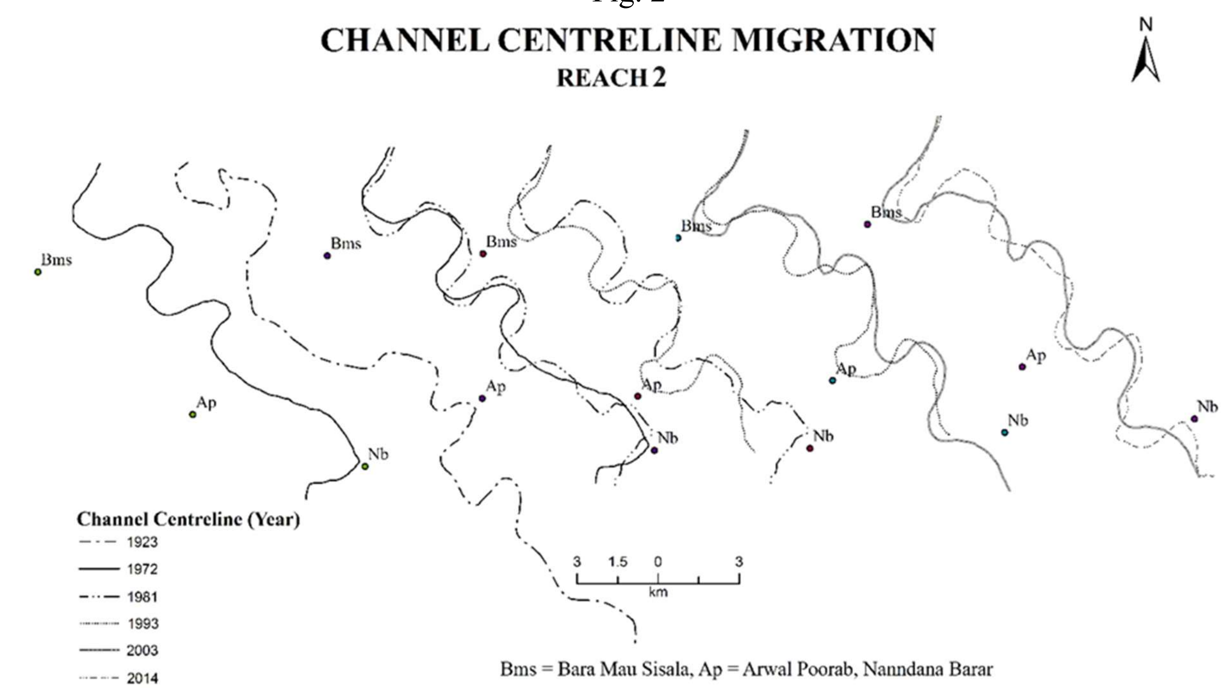

Fig. 3

CAHIERS MAGELLANES-NS
Volume 06 Issue 2
2024

ISSN:1624-1940
DOI 10.6084/m9.figshare.2632574
http://magellanes.com/

Bankline migration

The Ramganga river in the Western Gangetic Plain mostly shifts its channel east-west or west-east. Over several years, the Ramganga River's study reach shows varied degrees of bank movement and migration patterns. Extensive study of the bank line reveals different patterns and magnitudes of lateral migration.

In the reach 1, the right and left banks showed a clear eastward migratory pattern throughout the years 1923–1972 (Fig. 4). Table 2 shows the average eastward displacement of the right bank as 1,678.62 m; the left bank moved eastward by an average of 1,329.11 m. Intriguingly, an asymmetric lateral migration pattern was shown by the average westward movement of the right bank being 1.59 times higher than the left bank during the same timeframe.

Between 1972 and 1981, both bank lines showed almost consistent westward migratory tendency. The right and left banks' average westward extension came at 1,106.43 m and 1,295.61 m correspondingly. Large-scale channel movements over both sides were observed during this era; the largest westward migration noted for the right bank was 3,020.42 m and for the left bank was 3,808.06 m. The maximum limit of westward migration recorded as 3,020.42 m for the right and 3,808.056 m for the left bank respectively, the eastward extension of the right bank was notably 2.34 times higher than the left bank.

For both banks, the rate of westward bank line migration dropped considerably during the 1981–1993 period. For the right bank, the rate of eastward migration was 2.31 times larger than its westward movement, though. On the left bank, migration followed both eastward and westward directions in very similar fashion.

The right bank's westward migration increased significantly between 1993 and 2003 when compared to the decade before. The left bank's average eastward migration also showed a remarkable decline concurrently.

With an average migration rate of 5,767.38 m, the westward migration of the left bank grew remarkably in the years 2003–2014. Although the westward migration of the bank was seen during this time, the migration rate was far lower than that of the left bank.

The different trends of bank line migration recorded in the research emphasize the dynamic character of the Ramganga River and its inclination to change significantly over time. Alternating periods of dominance in eastward or westward directions, the asymmetric migration patterns imply the influence of local geomorphological elements and complicated hydrodynamic processes.

Examining the channel bank line migration patterns in the study reach 2 (Fig. 5) exposes notable lateral changes over several time periods, including cases of channel avulsion and desertion of prior courses.

The whole channel of the study reach shows an amazing westward movement between 1923 and 1972, therefore capturing the route of a tributary channel of the Ganga River called Kunda River. The Ramganga River thus began to veer off course and run through this tributary channel. The water has remarkably not returned its abandoned path for the past 44 years. During this period, the right and left banks averaged 4,537.27 m and 4,242.31 m respectively for westward extension (Table 3). The highest westward movement of the right bank was 7,318.48 m.

From 1972 to 1981, the migration pattern changed and both banks' eastward migration gained more importance. For the left and right banks respectively, the average rate of eastward migration was 601.71 m and 339.08 m. Still, during this time the right and left banks' maximum westward movement noted

CAHIERS MAGELLANES-NS
Volume 06 Issue 2
2024

ISSN:1624-1940
DOI 10.6084/m9.figshare.2632574
http://magellanes.com/

as 2,682.33 m and 539.39 m respectively.

Table 2: Bank line Migration of Reach 1

Transect	1923-1972		1972-1981		1981-1993		1993-2003		2003-2014	
No	RB	LB	RB	LB	RB	LB	RB	LB	RB	LB
1	-2134.28	1687.15	-516.58	747.52	190.83	-333.85	561.07	-867.88	130.72	-2878.93
2	-2681.67	3460.32	-648.84	723.18	-104.65	-10.42	826.32	-719.35	232.06	-3453.59
3	-3243.08	3502.20	-834.68	454.00	-50.48	591.51	-808.22	450.22	1865.81	-5186.30
4	-3762.40	4162.01	-227.91	178.96	-848.37	1210.70	-819.48	358.19	1997.87	-5670.89
5	-1648.49	1706.43	2760.82	-2214.65	-2412.84	1859.48	10.07	272.97	1858.23	-8551.85
6	-1460.02	1094.41	2920.04	-2576.11	-2318.36	2554.96	-550.48	10.91	-149.81	-8480.24
7	-1061.35	844.42	3020.42	-2633.83	-2180.64	2645.83	-1142.00	63.93	-110.98	-8244.31
8	-904.85	682.48	2865.38	-2488.16	-1986.17	2385.46	-1203.72	227.14	-150.88	-7856.62
9	-591.37	568.82	2419.80	-2211.63	-1588.85	2027.18	-1087.19	325.66	-283.82	-7502.43
10	-1034.38	639.13	1662.97	-511.42	-1117.53	407.77	-762.31	205.54	-338.81	-7267.95
11	-3418.42	3951.79	394.45	-264.99	-217.24	364.08	-316.42	-62.06	-167.43	-7101.23
12	-3304.18	3910.03	-411.95	-196.60	102.92	291.86	27.63	61.77	116.32	-7133.29
13	-2982.23	3650.91	-153.76	-239.70	-38.30	257.74	46.06	180.59	313.83	-7076.32
14	-466.54	659.29	-16.28	-222.07	-69.18	202.27	182.12	278.13	191.41	-7120.92
15	-246.99	412.22	92.72	-133.19	22.58	14.15	113.86	369.36	-222.58	-7373.77
16	-160.66	251.12	161.49	-32.72	179.13	-90.29	35.93	164.66	-754.34	-7724.95
17	266.68	93.96	-38.76	-131.93	273.39	112.07	326.76	-342.39	776.11	-7355.31
18	582.62	131.11	-762.71	57.79	263.54	-123.30	745.80	-	456.52	-

ISSN:1624-1940
DOI 10.6084/m9.figshare.2632574
http://magellanes.com/

								1090.52		6275.12
19	1841.41	220.58	-2594.91	469.69	205.78	-522.21	1009.78	-910.76	185.72	-3869.20
20	1481.64	-367.23	-2494.11	1582.05	312.40	-824.59	646.57	-94.02	400.19	-4294.97
21	399.15	-164.44	-1348.06	1284.61	290.96	-844.97	-57.12	555.50	1014.00	-5056.31
22	495.92	-260.99	-1129.83	801.24	323.33	-762.47	-284.58	508.01	1117.73	-5321.40
23	692.22	-631.60	-724.22	832.99	345.56	-688.27	-126.66	54.96	673.23	-5336.21
24	811.58	-797.24	26.58	241.28	-280.41	-69.55	373.92	-513.23	153.39	-5447.85
25	1803.43	-1457.61	597.41	-244.37	-536.77	350.21	413.63	-617.93	27.97	-5693.75
26	650.09	-691.04	1165.39	-914.32	-665.84	338.33	213.58	-235.85	439.67	-5474.27
27	-1078.69	489.66	1321.65	-1274.56	-419.48	266.05	1.99	119.37	903.87	-5608.80
28	-1769.76	1039.53	13.80	170.53	1183.56	-1553.07	-307.83	355.47	976.26	-5786.92
29	-2106.46	1118.65	74.87	247.20	1173.14	-2012.35	341.88	630.84	-170.02	-5920.30
30	-1979.49	673.55	181.79	642.81	983.89	-1934.24	872.32	-256.46	-1190.49	-5090.00
31	-1422.61	756.35	-43.42	150.95	692.05	-1237.83	900.70	-416.95	-1542.78	-5101.10
32	-1097.37	648.34	381.06	834.35	147.98	-1779.74	843.09	-492.77	-1345.86	-5046.81
33	-53.04	-964.22	441.72	2009.69	28.66	-185.11	773.47	623.53	-1125.63	-640.16
34	167.03	-521.33	519.73	2508.49	-236.47	-429.61	524.10	513.39	-512.65	-231.26
35	192.22	-1388.88	-303.13	3808.06	347.78	541.29	-152.08	-127.58	123.99	116.12
36	448.69	-1370.35	-5314.51	-224.30	95.43	-93.46	3934.03	4002.87	304.57	673.02
37	3439.59	-1164.17	-5105.49	-65.54	41.04	-31.35	-32.99	-4.55	-72.04	-27.81

The average degree of westward migration for both banks was far clearer in the next period, 1981–1993.

ISSN:1624-1940
DOI 10.6084/m9.figshare.2632574
http://magellanes.com/

The left and right banks shifted average eastward throughout this period: 536.60 m for the left and 376.62 m for the right. The right and left banks' maximum eastward expansion respectively came at 2,739.16 m and 1,666.14 m.

Over the years 1993 to 2003, banks' eastward migration dominated. For the right and left banks respectively, the maximum extent of eastward migration was 3,618.41 m and 3,394.16 m. Though the average extent of westward migration for the right bank was 349.22 m, westward migration was very obvious for the left bank with an average extent of 1,777.12 m.

Whereas the average eastward extent of the left bank was 5.58 times higher than the right bank, the average extent of westward migration was somewhat noticeable for the right bank during the period 2003–2014. Whereas the average eastward migration was 148.46 m for the right bank and 828.18 m for the left bank, the average extent of westward migration for the right and left banks was 944.77 m and 716.76 m respectively.

The observed channel migration patterns underline the dynamic character of the Ramganga River and its inclination to experience major lateral changes including avulsions and the abandoning of historical courses. Along with the different migration distances, the alternating periods of dominance in eastward or westward migration imply the influence of complicated hydrodynamic processes, sediment dynamics, and local geomorphological influences.

Table 3: Bank line Migration of Reach 2

Transect No	1923-1972		1972-1981		1981-1993		1993-2003		2003-2014	
	RB	LB	RB	LB	RB	LB	RB	LB	RB	LB
1	3082.26	-3100.83	616.64	190.22	-727.68	-0.32	-392.73	107.46	-22.70	40.99
2	3369.48	-3057.25	354.17	314.70	-752.24	46.76	-276.14	47.42	-55.93	48.69
3	3853.65	-3622.36	-67.15	269.57	-499.21	128.76	-201.40	72.58	-26.25	73.70
4	5354.64	-5439.10	-198.55	110.14	-250.32	258.49	-18.29	62.58	-177.85	108.55
5	7318.48	-6842.46	-6.05	-13.91	-28.77	-309.35	68.28	147.25	-119.42	2107.55
6	6710.50	-3986.30	253.42	43.91	388.49	-3228.08	76.80	-164.44	109.13	3277.02
7	3605.14	-3259.1	2682.33	152.27	635.12	-1422.13	356.14	-2947.0	118.09	3956.54

ISSN:1624-1940
DOI 10.6084/m9.figshare.2632574
http://magellanes.com/

		2						4		
8	3086.48	-3043.49	-144.39	257.73	3215.43	-927.70	840.12	-3264.74	433.09	3641.08
9	3313.07	-3132.38	-467.49	634.83	934.94	-977.35	-1032.40	812.21	4709.61	-585.04
10	3697.96	-3100.25	-684.68	462.75	847.13	-994.51	-1070.37	1056.50	385.06	-253.92
11	3858.86	-3017.46	-381.04	-147.50	445.58	-258.84	-1176.41	2488.73	-225.89	-874.30
12	3720.52	-2985.09	100.12	61.03	-2739.16	1666.14	465.98	29.10	85.34	-408.40
13	2387.81	-2468.54	-386.36	592.10	-156.26	-41.18	419.53	37.14	10.65	137.12
14	3134.73	-3230.30	-380.53	517.92	-333.51	28.05	-17.33	110.23	-5.56	180.90
15	3631.06	-3828.09	65.10	88.82	-369.91	414.41	-409.30	85.52	8.68	51.51
16	5128.54	-5294.44	597.58	-12.13	-32.21	93.70	-887.65	313.08	92.29	57.59
17	7121.33	-7096.51	953.14	805.48	412.95	-1774.62	-1199.58	791.26	281.16	50.80
18	6091.76	-4722.18	-514.34	-539.39	2887.67	-3019.84	-3618.41	3394.16	2428.34	-2070.38
19	5119.90	-5786.96	516.10	-101.23	-13.28	-718.67	-423.17	310.87	2318.21	227.31
20	5700.95	-4974.38	471.92	304.47	134.18	-1614.98	17.03	176.53	-255.24	335.66

CAHIERS MAGELLANES-NS
Volume 06 Issue 2
2024

ISSN:1624-1940
DOI 10.6084/m9.figshare.2632574
http://magellanes.com/

21	4866.31	-4292.21	8.32	341.32	976.90	-2003.63	189.29	-134.64	-280.34	362.31
22	4337.63	-3422.08	-991.84	318.03	1933.01	-2220.05	455.59	-396.22	-154.91	215.85
23	4245.25	-3107.29	-734.70	132.45	1688.46	-2182.23	603.45	-155.61	-52.50	-108.51
24	4831.28	-6082.39	-456.03	-380.51					422.10	1062.51
25	5864.15	-7166.33	-982.82	844.75					1825.06	656.91
26									-459.73	545.37
27									-93.73	253.76

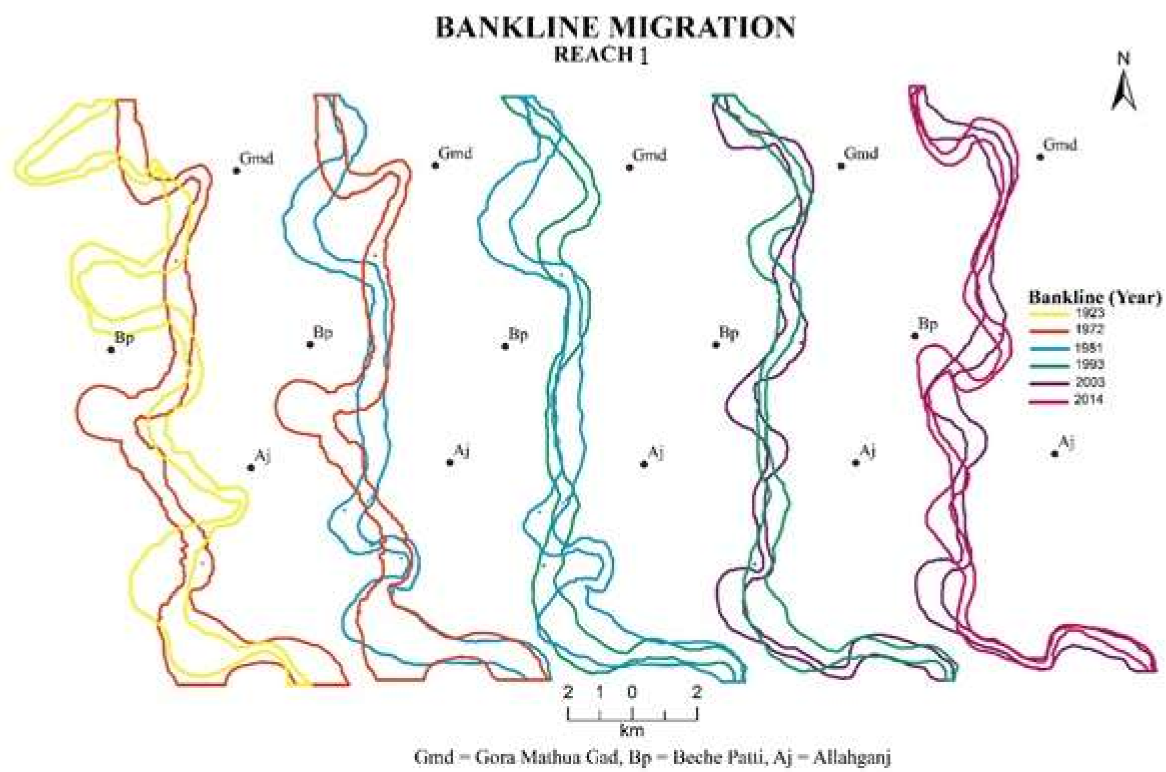

Fig. 4

CAHIERS MAGELLANES-NS
Volume 06 Issue 2
2024

ISSN:1624-1940
DOI 10.6084/m9.figshare.2632574
http://magellanes.com/

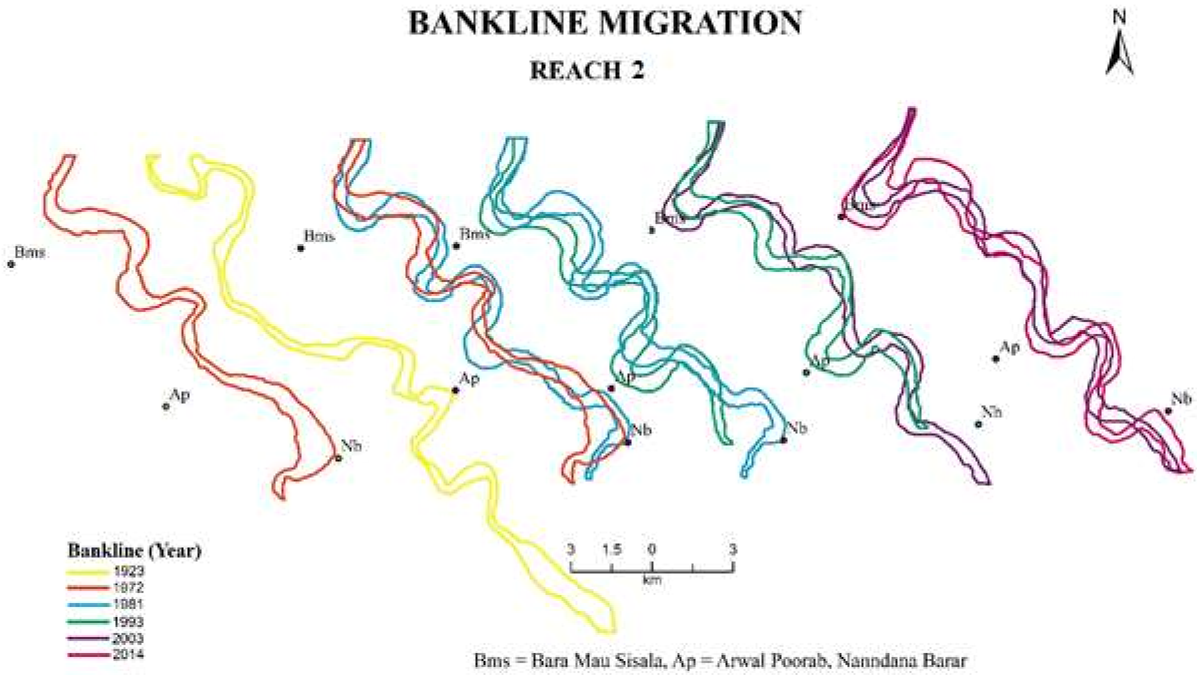

Fig. 5

Morphodynamics of Channels

Active Channel Width (ACW)

Active channel width of a river is that section of the river whose complete portion is occupied by the wet channel within both riverbanks. In the reach 1, a notable amount of temporal shift in ACW was noticed (Fig. 6. i). Although 1923 had the greatest mean ACW (331.9 m), it dropped by -15.95 per cent in the next period, 1972. While it dropped (-38.37%) sharply in 1993 compared to the 1981 era, the mean ACW somewhat raised (5.37%) in 1981 compared to the previous period. Up to 2014, mean ACW showed a declining trend. Tributary channels supplied water to the Ramganga River throughout the year, therefore preserving a constant flow of water. In case of reach 2,1923 had the highest mean ACW (264.33 m), followed by declining values in the next years; in 2014, it dropped to 185.78 m. In every period, the value of Coefficient of Variation (CV) reduced from 0.25 in 1923 to 0.31 in 2003. Consequently, the rate of fluctuations in ACW at the geographical and temporal scales was not rather important. The volume of water discharge in this reach was higher as, as it is known, before getting into the present study reach, all of the tributaries of the Ramganga River (excluding Deoha River) supplied water to Ramganga (Fig 6.ii).

CAHIERS MAGELLANES-NS
Volume 06 Issue 2
2024

ISSN:1624-1940
DOI 10.6084/m9.figshare.2632574
http://magellanes.com/

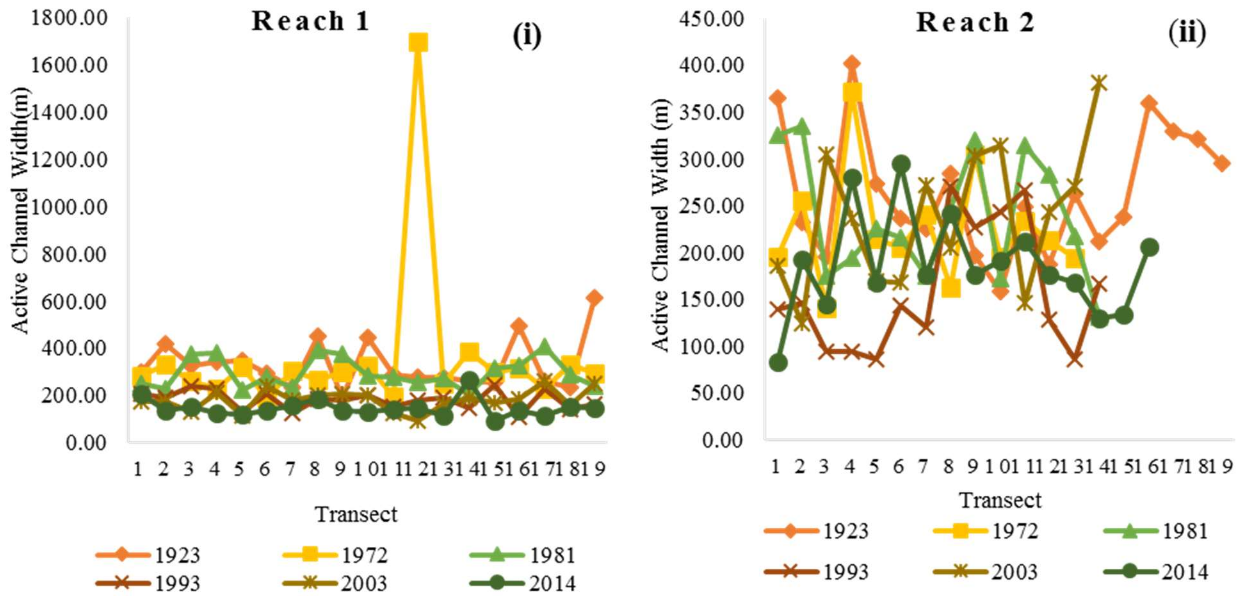

Fig. 6

Channel Length (CL)

The channel length (CL) is the longitudinal distance between the two places. Apart from spatial direction, the channel length varies temporally within reach. Whereas the river straightens its path by neck cut-off or chute cutoff, the channel length increases as the channel curvature rises. The alluvial reach from the river stream varied significantly depending on the channel length. In reach 1 the year 1923 (40.97 km) showed the highest CL (Fig. 7.i), however, it declined slowly in the succeeding years. The CL fell 5.8 km between 1923 and 2014 with a rate of 61.37 m/year. The temporal scale lets the length of the channel change dramatically. Except between 1972 and 1981, the CL show a noteworthy annual pace of change. In 1923, the Ramganga channel displayed a quite meandering route. As so, the channel length rose in relation to the other observed periods. Though numerous more meander bends developed, the course's length fell by 10.06 km, and the channel straightened its direction by a cut in 1972. Within the decadal time scale, the length of the route displayed a notable decline in 1993–2003 (2.988 km); in the next period, the length of the CL showed a remarkable increase (3.72 km).

ISSN:1624-1940
DOI 10.6084/m9.figshare.2632574
http://magellanes.com/

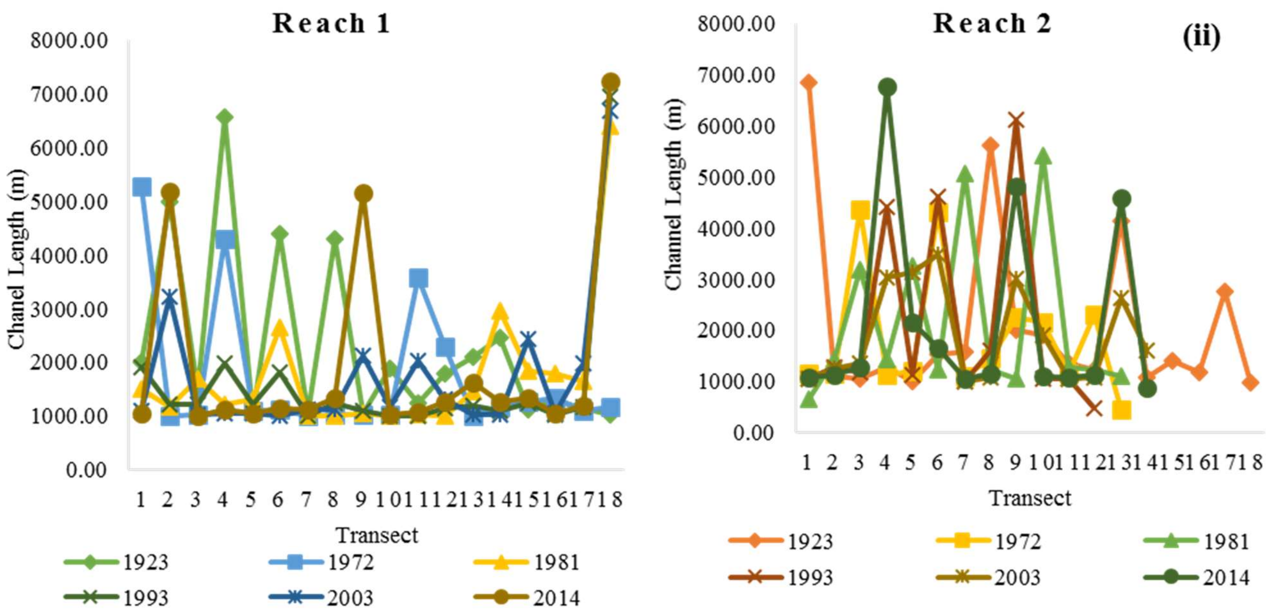

Fig. 7

Further complex growth of the meander bend improved the bend curvature, hence aggravating the channel's length during 1972–1981 (98.64). In 1923–1972, the CL declined to 10.01 km; in 1972–1981, it somewhat raised (0.89 km). Between 1981 and 1993, the CL declined dramatically (-3.19 km); between 1993 and 2014, it grew noticeably (6.73 km).

In the reach 2, difference in channel length mainly attributed with the shifting confluence of the Ganga and the Ramganga rivers (Fig. 7.ii). In 1923, the CL of this section was 39.98 km; in 1972, it declined 13.79 km from the previous year. Between 1923 and 1972, the Ramganga River veered off course and left its main path behind and established its new course on Kunda Nala, a tributary stream of the Ramganga river. As a result, the juncture of the Ramganga and the Ganga rivers relocated further west, drastically lowering the CL of the former river. The Ramganga river had not returned to its native course since 1972 having been traversing the Kunda Nala. Major alternations in CL between 1972 and 2014 were from meander bend extension or cut-off as a change in the confluence point. Between 1972 and 1981, the CL rose 3.36 km; between 1981 and 1993, it plummeted to 2.57 km. Once more, in 1993–2003, the CL increased (1.76km), then maintained on till 2003–2014. With a yearly rate of change in CL of 291.67 m/year, 1972–1981 (372.83 m/year) had the highest rate. The confluence point between the Ramganga and the Ganga rivers migrating northwest between 1981 and 1993 produced attenuation of CL. The length of the channel steadily expanded for two reasons between 1993 and 2014: the extension of the meander bend and south-eastward confluence shifting.

Channel Sinuosity (CS)

The channel sinuosity accounted higher in amount than any other upstream reaches in the reach 1. The Ramganga River here exhibited a truly meandering course. The channel sinuosity of this reach was remarkably higher in 1923 (2.26). During 91 years of study, the CS was reduced by -15.32 per cent. The CS drastically subdued (-23.91%) in 1972 than the preceding period but it remained relatively unchanged in 1972-1981. In 1981-1993, the CS again decreased by -10.4 percent. In contrast, since

CAHIERS MAGELLANES-NS
Volume 06 Issue 2
2024

ISSN:1624-1940
DOI 10.6084/m9.figshare.2632574
http://magellanes.com/

1993, the CS has started to increase. During 1993-2003, the CS increased by 10.41 percent and this trend further continued in the subsequent decade. In 2014, the channel sinuosity became very high, i.e. 1.92 (Fig. 8.ii).

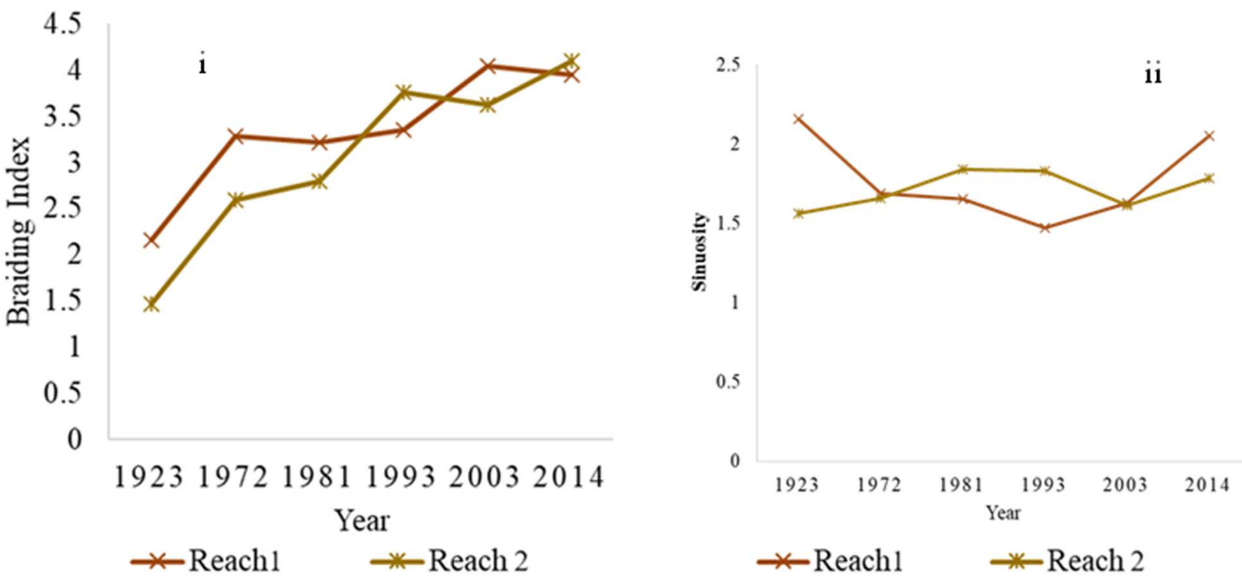

Fig. 8 i. Braiding Index, ii. Sinuosity

The Ramganga River exhibited remarkably greater sinuosity in the reach 2. The changes in the confluence point between the Ramganga and the Ganga rivers at different periods adversely affected the sinuosity of the study area. Between 1923 and 1972 period, the Ramganga River changed its course and met the Ganga River further upstream from the previous confluence point. Although the length of the channel significantly reduced the channel sinuosity increased in 1972 by 9.35 percent compared to 1923 CS. From 1972-1993, the channel sinuosity increased from 1.79 to 1.98. In this period, the main causes of increasing sinuosity were the meander bend extension, translation and rotation. During 1993-2003, the CS decreased by -12.24 per cent, while it increased again (9.97%) during 2003-2014. Since the last 91 years of study, Channel Sinuosity increased by 16.30 per cent.

Due to the variations in the confluence between the Ramganga and the Ganga rivers, the channel oscillated from its previous position, causing the channel to be absent in some of the sections. However, the section wise channel sinuosity largely varies temporally as well as spatially.

Braiding Index (BI)

The braiding index increased remarkably between 1923-2014 in the reach 1. Within the entire assessed period, the BI increased by 82.45 per cent. In 2014, the channel showed a tendency to be intensely braided. Along with this, a major increase in BI was observed between 1923 and 1972 (51.63%). In this period, the river transformed from partly braided to moderately braided river. During 1972-1993, the channel exhibited the features of moderately braided streams. However, in 2003-2014 it showed the indication of the intensely braided characteristics.

In 1923, in the topographical map, the Ramganga river along this study reach exhibited the

ISSN:1624-1940
DOI 10.6084/m9.figshare.2632574
http://magellanes.com/

characteristics of a single thread channel (BI= 1.46), but after the major channel avulsion that took place between 1923 to 1972 period, the tendency of the braiding of the Ramganga increased profoundly in the reach 2. The rapid increase in the BI was noted during 1981-1993 (34.57%). In 2014, the river with a very high BI (4.10) indicated the characteristics of the intensely braided river (Fig. 8.i).

Active Channel Area (ACA)

Active channel area refers to the total area of a river that comes under the region of continuous water discharge. Within the entire evaluated period, the active channel area decreased by -62.51 per cent in the reach 1. From 1923 to 1993, the ACA reduced persistently, but in 1993-2003, it increased by 20.53 percent. During 2003-2014, the active channel area decreased (-20.69%) again. The highest rate of change in CBA was observed in 1981-1993 (-45.12%), while it was minimal in 1972-1981 (10.44%). During 1923-1972, 1993-2003 and 2003-2014, the changes in active channel area were detected in a similar fashion (Fig. 9.i). In these decades, the change was ~20 per cent more than the preceding decade. In the study reach 2, the active channel area varies due to changes in the confluence point that lead to changes in the channel length (Fig. 9.ii). In 1923, the active channel area was 80, 64,931.64 m². It registered the highest among all of the studied periods. The ACA drastically reduced to 52 06,097.73 m² in 1972 as the confluence shifted towards the further west and the channel length decreased momentously. The lowest ACA was observed during 1993 as from 1981 to 1993, the Ganga River shifted towards the north the new confluence point was set up in an upstream portion between the Ramganga and the Ganga. Because of that, the channel length and the active channel area of Ramganga were reduced accordingly. Since the last 91 years, the ACA reduced by -40.74 per cent. The maximum variation in the active channel area was observed in 1993-2003 (45.23%), followed by 1923-1972 (-35.45%) and 1981-1993 (-30.15%). During 1972-1981 and 2003-2014, some of the considerable changes were also observed.

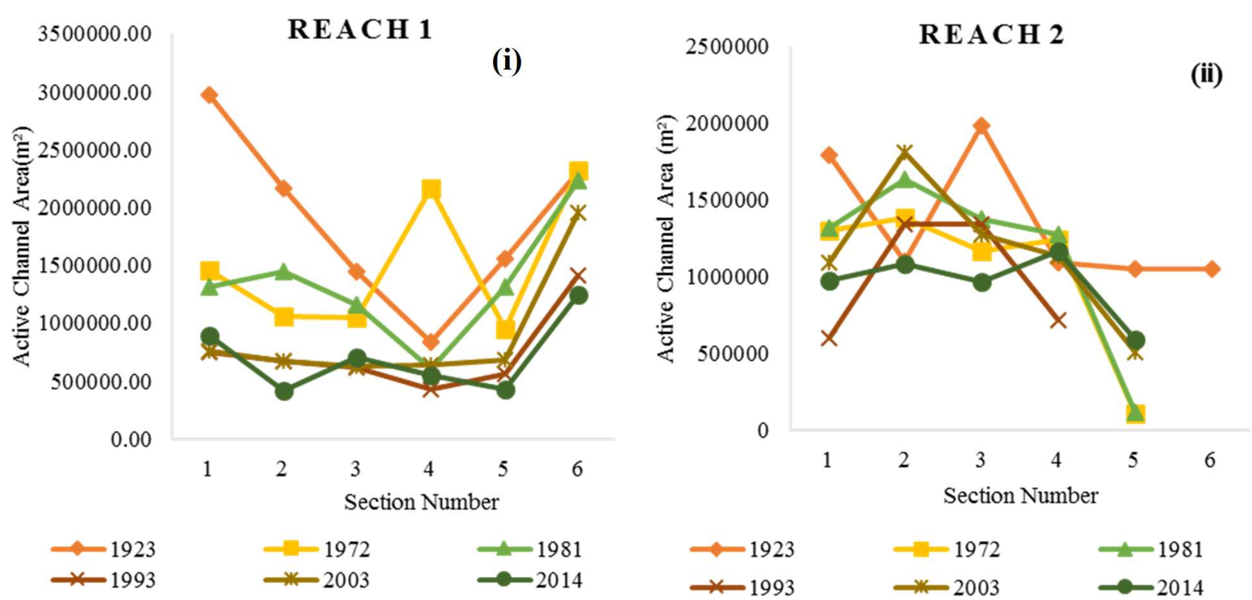

Fig. 9

CAHIERS MAGELLANES-NS
Volume 06 Issue 2
2024

ISSN:1624-1940
DOI 10.6084/m9.figshare.2632574
http://magellanes.com/

Channel Belt Area (CBA)

The channel belt area is the total area of the channel within which the channel has laterally migrated after its existence, showing its maximum extension since the channel originated. It represents the farthest areal limit of the channel lying on both sides of the present channel where the channel moves laterally.

In reach 1 the channel belt area has been increasing since 1923 in the reach 1(Fig. 10.i). In 1923, the CBA was 13, 66, 91,466.79 m², but it increased up to 16, 99, 74,902.46 m² in year 2014. It was noticed that during the entire period of study, the CBA increased by 24.35 per cent. The decadal variations of CBA were not so prominent in the decadal time scale. Only some significant changes occurred in 1923-1972 (21.26%) and 2003-2014 (-20.70%), but since 1972-2003 only ~ 1 per cent change was discerned.

In the reach 2, within entire assessed periods, some striking variations in the channel belt area were observed. During 1923, the total CBA of that study area was 2,01,22,150.22 m², but in 1972 it had increased manifolds (409.04%) than to 1923, as the Ramganga river setup its new channel towards the west while abandoning its old course. After 1972, the major variation in the CBA was observed during 1993-2003 (72.46%), but in other decades there were no notable temporal changes in CBA was experienced (Fig 10.ii).

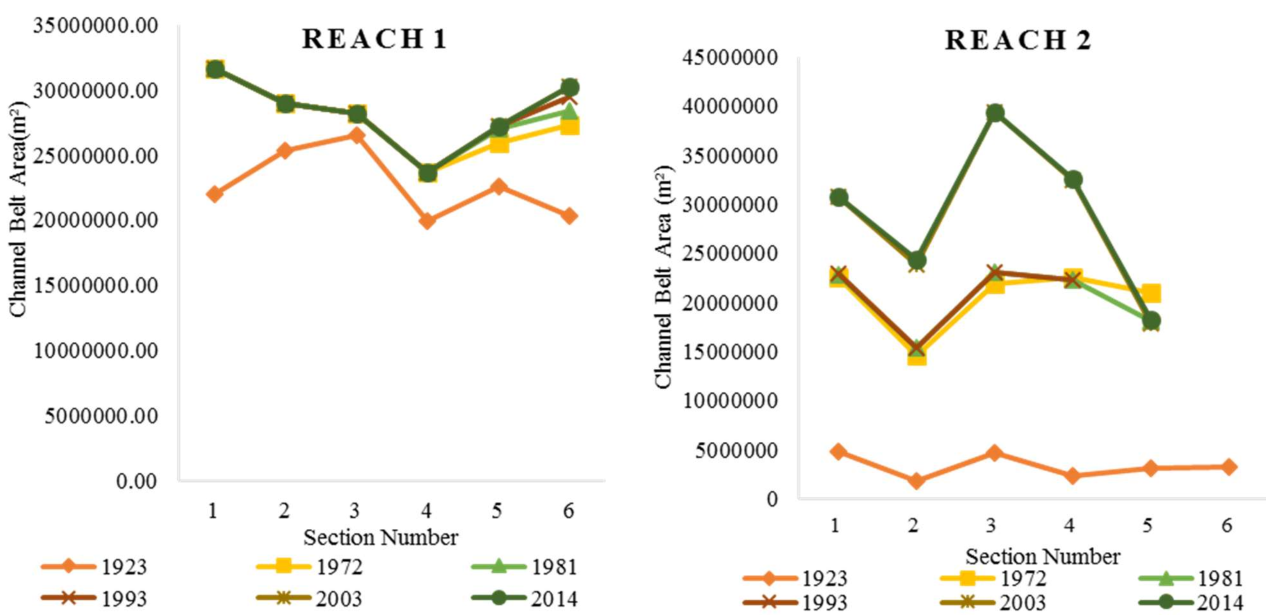

Fig. 10

Active Channel area Channel belt area Ratio (ACACBAR)

The ACACBAR registered highest in 1923 (0.40), but the ratio reduced momentously in 1972 (-87.32%) (Fig.11). As the channel belt area increased by 409.04 per cent in 1972 compared to the previous period, the ratio had decreased consequently. From 1923-2014, the ratio decreased by -91.80 percent. From 1972-2014, a small amount of change, ~15percent, was observed.

CAHIERS MAGELLANES-NS
Volume 06 Issue 2
2024

ISSN:1624-1940
DOI 10.6084/m9.figshare.2632574
http://magellanes.com/

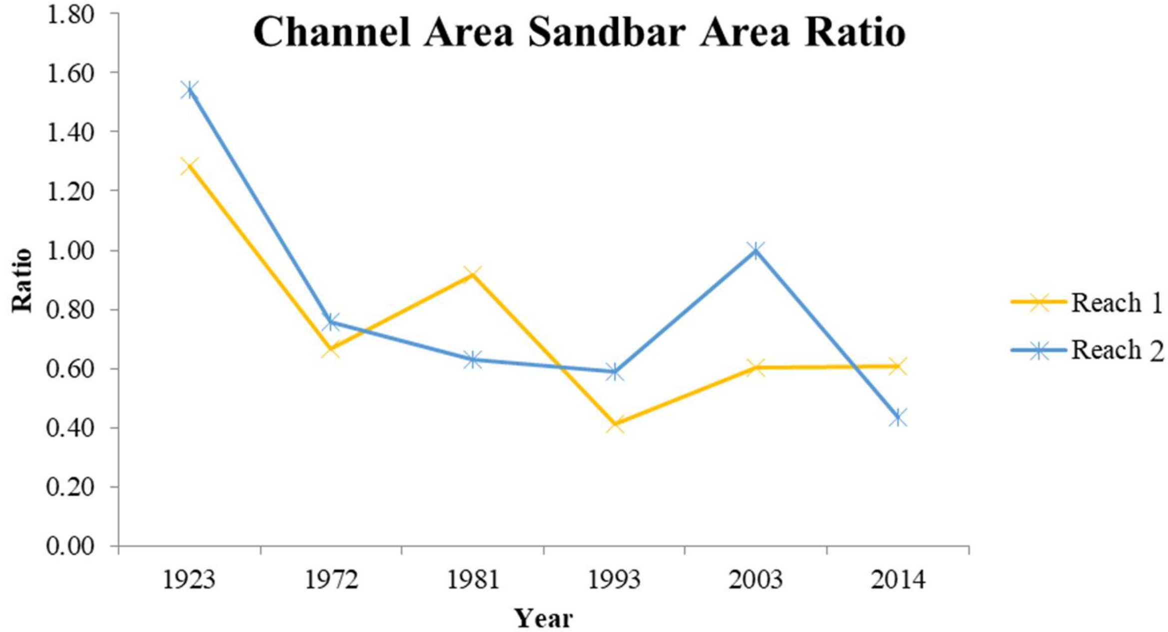

Fig. 11

Total Sandbar Area Channel Area Ratio (TSACSR)

It is defined as the ratio between the total sandbar area and the total channel area within a definite reach. Along the reach 1, the channel area was higher than the sandbar area in 1923 (0.81). The highest value of this ratio was observed only in 1993 (2.77). In this regard, the sandbar accretion has increased remarkably since 1993 (Fig. 12.i). As a result, the degree of braiding had increased manifolds. Along the reach 2, the accretion of the sand had accentuated after the channel avulsion that occurred during 1923-1972. The maximum amount of this ratio was observed in 2014, which occurred due to the rapid rate of increase in the sand bar area as well as the reduction in the channel area (Fig. 12.ii).

CAHIERS MAGELLANES-NS
Volume 06 Issue 2
2024

ISSN:1624-1940
DOI 10.6084/m9.figshare.2632574
http://magellanes.com/

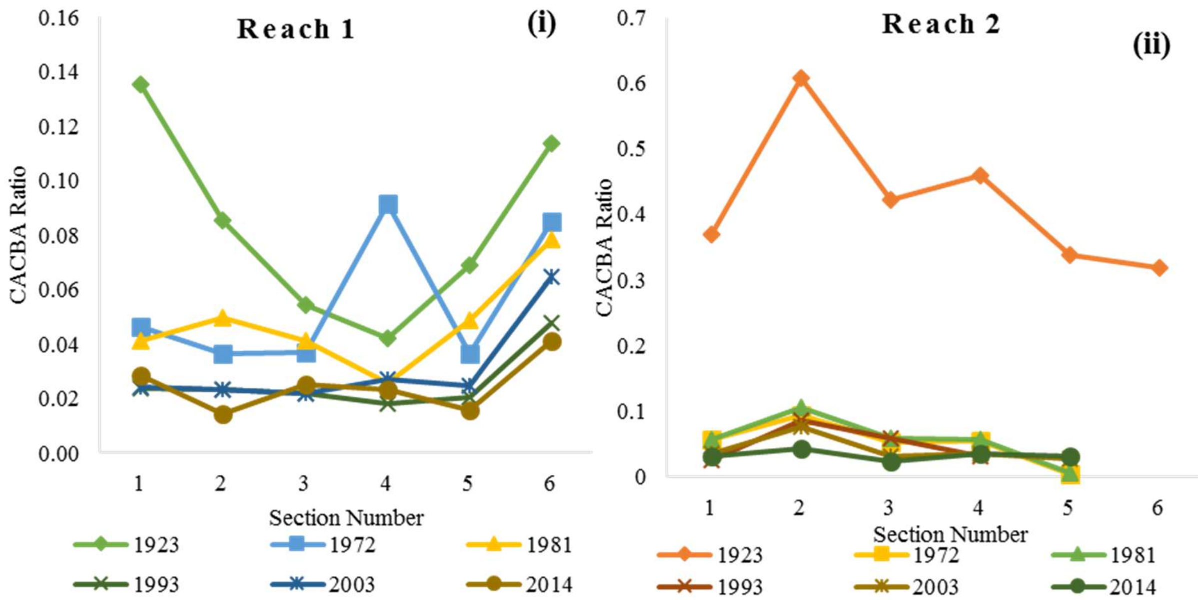

Fig. 12

Conclusion

The study involves the quantification of the morphological changes and lateral movement patterns of the Ramganga River during the past century (1923-2014) based on multi-temporal analysis of remotely sensed data and topographic maps. It showed the Ramganga River has experienced significant channel modifications in the past century. Several morphological parameters, including channel width, sinuosity, braiding intensity, active channel area, channel belt area, and sandbar accretion, were taken into consideration which show spatio-temporal variations which help to understand the complex mechanisms controlling channel development and behaviour. With a decrease in active channel width and area over all investigated lengths, the study reveals that the active channel area of the Ramganga River has been diminishing. Concurrently, the channel has exhibited increasing tendency for braiding; the braiding index shifts from single-thread to substantially braided patterns in several reaches over the research period.

Furthermore, the meander bend evolution, cut off events, and avulsions have shaped the channel sinuosity; it has also changed most strikingly in alternating stages of increasing and decreasing sinuosity. Mostly under effect of modifications in meander curvature, cut-offs, and confluence position with the Ganga River, notable channel length variations were observed.

The study also demonstrated the dynamic character of the channel belt area—which has expanded significantly in some reaches by means of lateral migration and avulsion of the channel is underlined in the study. The active channel area to channel belt area ratio has reduced with time, implying increasing inclination for lateral motion and the development of abandoned channels and floodplain features.

Additionally, the analysis of bank line migration patterns reveals alternately dominant eastward or westward migration with sporadic major channel avulsions and abandoned former pathways. The observed asymmetric migration patterns suggest the existence of complex hydrodynamic mechanisms and local geomorphological constraints.

Finally, the remote sensing data, GIS techniques, and field observations combined greatly helped to

ISSN:1624-1940
DOI 10.6084/m9.figshare.2632574
http://magellanes.com/

reconstruct the historical channel morphodynamics and trace out the driving factors. Nevertheless, the limits of the present data sources and the natural complexity of fluvial processes underline the need of continuous data collecting, improved modelling capacity, and multi-disciplinary research projects.

Acknowledgements: The first author acknowledges University Grants Commission (UGC), New Delhi, India for financial assistance. The authors are highly grateful to the Department of Geography, BHU, for providing necessary facilities for doing this research.

References

Agnihotri, A. K., Ohri, A., & Mishra, S. (2020). Channel planform dynamics of lower Ramganga River, Ganga basin, GIS and remote sensing analyses. Geocarto International, 35(9), 934–953.

Akhter, S., Eibek, K. U., Islam, S., Islam, A. R. M. T., Chu, R., & Shuanghe, S. (2019). Predicting spatiotemporal changes of channel morphology in the reach of Teesta River, Bangladesh using GIS and ARIMA modeling. Quaternary International, 513, 80–94.

Anderson, M. G., & Calver, A. (1980). Channel plan changes following large floods. In R. A. Cullingford, D. A. Davidson, & J. Lewin (Eds.), Timescales in Geomorphology (pp. 43–52). Wiley.

Arnaud, F., Piégay, H., Schmitt, L., Rollet, A. J., Ferrier, V., & Béal, D. (2015). Historical geomorphic analysis (1932–2011) of a by-passed river reach in process-based restoration perspectives: The Old Rhine downstream of the Kembs diversion dam (France, Germany). Geomorphology, 236, 163–177.

Ashmore, P., & Church, M. (2001). The impacts of climate change on rivers and river processes in Canada. Geological Survey of Canada Bulletin.

Baki, A. B. M., & Gan, T. Y. (2012). Riverbank migration and island dynamics of the braided Jamuna River of the Ganges-Brahmaputra basin using multi-temporal Landsat images. Quaternary International, 263, 148–161.

Baldwin, W. E., Morton, R. A., Putney, T. R., Katuna, M. S., & Gayes, P. T. (2006). Migration of the Pee Dee river system inferred from ancestral palaeochannels underlying the South Carolina Grand Strand and Long Bay inner shelf. Geological Society of America Bulletin, 118(5-6), 533-549.

Bandyopadhyay, S., Ghosh, K., & De, S. K. (2014). A proposed method of bank erosion vulnerability zonation and its application on the River Haora, Tripura, India. Geomorphology, 224, 111-121.

Bartley, R., Keen, R. J., Hawdon, A. A., Hairsine, P. B., Disher, M. G., & Kinsey-Henderson, A. E. (2008). Bank erosion and channel width change in a tropical catchment. Earth Surface Processes and Landforms, 33, 2174–2200.

ISSN:1624-1940
DOI 10.6084/m9.figshare.2632574
http://magellanes.com/

Bertoldi, W., Zanoni, L., & Tubino, M. (2009). Planform dynamics of braided streams. Earth Surface Processes and Landforms, 34(4), 547-557.

Bhakal, L., Dubey, B., & Sarma, A. K. (2005). Estimation of bank erosion in the river Brahmaputra near Agyathuri by using geographic information system. Journal of the Indian Society of Remote Sensing, 33(1), 81–84.

Bhowmik, M., & Pan, N. D. (2014). Qualitative assessment of bank erosion hazard in a part of the Haora River, West Tripura District. In M. Singh (Ed.), Landscape ecology and water management (pp. 193–203). Springer.

Brice, J. C. (1964). Channel patterns and terraces of the Loup rivers in Nebraska. United States Geological Survey Professional Paper, P 0422-D, D1–D41.

Brierley, G. J., & Fryirs, K. A. (2013). Geomorphology and river management: applications of the river styles framework. John Wiley & Sons.

Chang, H. H. (2008). River morphology and river channel changes. Transactions of Tianjin University, 14, 254–262.

Clerici, A., Perego, S., Chelli, A., & Tellini, C. (2015). Morphological changes of the floodplain reach of the Taro River (Northern Italy) in the last two centuries. Journal of Hydrology, 527, 1106-1122.

Das, A. K., Sah, R. K., & Hazarika, N. (2012). Bankline change and the facets of riverine hazards in the floodplain of Subansiri–Ranganadi Doab, Brahmaputra Valley, India. Natural Hazards, 64, 1015–1028.

Feng, X., Zhang, G., & Yin, X. (2011). Hydrological responses to climate change in Nenjiang River basin, North-eastern China. Water Resources Management, 25, 677–689.

Ghimire, S., & Higaki, D. (2015). Dynamic river morphology due to land use change and erosion mitigation measures in a degrading catchment in the Siwalik Hills, Nepal. International Journal of River Basin Management, 13(1), 27-39.

Goswami, U., Sharma, J. N., & Patgiri, A. D. (1999). River channel changes of the Subansiri in Assam, India. Geomorphology, 30, 227-244.

Grant, G. E., Schmidt, J. C., & Lewis, S. L. (2003). A geological framework for interpreting downstream effects of dams on rivers. In J. E. O'Connor & G. E. Grant (Eds.), A Peculiar River: Geology, Geomorphology, and Hydrology of the Deschutes River, Oregon (pp. 203–219). American Geophysical Union.

ISSN:1624-1940
DOI 10.6084/m9.figshare.2632574
http://magellanes.com/

Grove, J. R., Croke, J., & Thompson, C. (2013). Quantifying different riverbank erosion processes during an extreme flood event. Earth Surface Processes and Landforms, 38, 1393–1406.

Cao, G. (2009). Channel sedimentation and erosion of the Jiangsu reach of the Yangtze River during the last 44 years. Earth Surface Processes and Landforms, 34, 1587–1593.

Guo, X., Gao, P., & Li, Z. (2021). Morphological characteristics and changes of two meandering rivers in the Qinghai-Tibet Plateau, China. Geomorphology, 379, 107626.

Gurnell, A. M., Downward, S. R., & Jones, R. (1994). Channel planform change on the River Dee meanders, 1976–1992. Regulated Rivers: Research & Management, 9, 187–204.

Halder, A., & Mowla Chowdhury, R. (2021). Evaluation of the river Padma morphological transition in the central Bangladesh using GIS and remote sensing techniques. International Journal of River Basin Management, 1–15.

Hickin, E. J., & Nanson, G. C. (1975). The character of channel migration on the Beatton river, Northeast British Columbia, Canada. Geological Society of America Bulletin, 86, 487-494.

Hickin, E. J., & Nanson, G. C. (1984). Lateral migration rates of river bends. Journal of Hydraulic Engineering, 110, 1557–1567.

Hooke, J. M. (1980). Magnitude and distribution of rates of river bank erosion. Earth Surface Processes, 5, 143–157.

Hossain, M. M. (1992). Total sediment load in the lower Ganges and Jamuna. Journal of the Institution of Engineers Bangladesh, 20(1–2), 1–8.

Jia, D., Shao, X., Wang, H., & Zhou, G. (2010). Three-dimensional modeling of bank erosion and morphological changes in the Shishou bend of the middle Yangtze River. Advances in Water Resources, 33, 348–360.

Karwan, D. L., Allan, J. D., & Bergen, K. M. (2001). Changing near-stream land use and river channel morphology in the Venezuelan Andes. Journal of the American Water Resources Association, 37(6), 1579-1587.

Khan, A. U., & Rawat, B. P. (1992). Quaternary geology and geomorphology of a part of Ganga basin in parts of Bareilly, Badaun, Shahjahanpur and Pilibhit district, Uttar Pradesh. G.S.I.

Khan, A., Rao, L., Yunus, A. P., & Govil, H. (2018). Characterization of channel planform features and sinuosity indices in parts of Yamuna River flood plain using remote sensing and GIS techniques. Arabian Journal of Geosciences, 11, 525.

ISSN:1624-1940
DOI 10.6084/m9.figshare.2632574
http://magellanes.com/

Khan, N. S., Roy, S. K., Mazumder, M. T. R., Talukdar, S., & Mallick, J. (2022). Assessing the long-term planform dynamics of Ganges–Jamuna confluence with the aid of remote sensing and GIS. Natural Hazards, 114(1), 883-906.

Kiss, T., & Blanka, V. (2012). River channel response to climate and human induced hydrological changes: Case study on the meandering Hernad River, Hungary. Geomorphology, 175-176, 115-125.

Knighton, A. D. (1973). Riverbank erosion in relation to stream flow conditions, River Bollin-Dean, Cheshire. East Midland Geographer, 5, 416–426.

Knighton, A. D. (1984). Fluvial forms and processes. Edward Arnold.

Morisawa, M. (1985). Rivers: forms and processes. Longman.

Kotoky, P., Bezbaruah, D., Baruah, J., & Sharma, J. N. (2005). Nature of bank erosion along the Brahmaputra river channel, Assam, India. Current Science, 88(4), 634–640.

Kummu, M., Lu, X. X., Rasphone, A., Sarkkula, J., & Koponen, J. (2008). Riverbank changes along the Mekong River: Remote sensing detection in the Vientiane–Nong Khai area. Quaternary International, 186(1), 100–112.

Lawler, D. M., Couperthwaite, J., Bull, L. J., & Harris, N. M. (1997). Bank erosion events and processes in the Upper Severn basin. Hydrology and Earth System Sciences, 1(3), 523–534.

Leopold, L. B., Wolman, M. G., & Miller, J. P. (1964). Fluvial processes in geomorphology. W. H. Freeman & Sons.

Lewin, J. (1972). Late-stage meander growth. Nature Physical Science, 240, 116.

Lewin, J. (1977). Channel pattern changes. In K. J. Gregory (Ed.), River channel change (pp. 167-184). John Wiley & Sons.

Mahmud, M. I., Mia, A. J., Islam, M. A., Peas, M. H., Farazi, A. H., & Akhter, S. H. (2020). Assessing bank dynamics of the Lower Meghna River in Bangladesh: an integrated GIS-DSAS approach. Arabian Journal of Geosciences, 13(14), 1–19.

Majumdar, S., & Mandal, S. (2020). Assessment of relationship of braiding intensities with stream power and bank erosion rate through Plan Form Index (PFI) method: a study on selected reaches of the upstream of Ganga river near Malda district, West Bengal, India. Sustainable Water Resources Management, 6(6), 1–18.

ISSN:1624-1940
DOI 10.6084/m9.figshare.2632574
http://magellanes.com/

Mandarino, A., Pepe, G., Maerker, M., Cevasco, A., & Brandolini, P. (2020). Short-term GIS analysis for the assessment of the recent active-channel planform adjustments in a widening, highly altered river: The Scrivia River, Italy. Water, 12(2), 514.

Micheli, E. R., & Larsen, E. W. (2011). River channel cutoff dynamics, Sacramento River, California, USA. River Research and Applications, 27, 328–344.

Midha, N., & Mathur, P. K. (2014). Channel characteristics and planform dynamics in the Indian Terai, Sharda River. Environmental Management, 53(1), 120–134.

Mukherjee, R. (2022). Quantitative assessment of channel planform dynamics and meander bend evolution of the Ramganga River, Ganga Basin, India. In Drainage Basin Dynamics: An Introduction to Morphology, Landscape and Modelling (pp. 89-113).

Mukherjee, R., Bilas, R., Biswas, S. S., & Pal, R. (2017). Bank erosion and accretion dynamics explored by GIS techniques in lower Ramganga river, Uttar Pradesh, India. Spatial Information Research, 25(1), 23-38.

Mukherjee, R., & Deb, P. (2024). Application of GIS-based analytical hierarchy process for assessment and mapping of flood risk zone in the lower Ramganga River Basin, Western Gangetic Plain, India. Environment, Development and Sustainability, 26 (3), 6163-6193.

Nanson, G. C., & Knighton, A. D. (1996). Anabranching Rivers: their cause, character and classification. Earth Surface Processes and Landforms, 21, 217–239.

Nardi, L., Campo, L., & Rinaldi, M. (2013). Quantification of riverbank erosion and application in risk analysis. Natural Hazards, 69, 869–887.

Nawfee, S. M., Dewan, A., & Rashid, T. (2018). Integrating subsurface stratigraphic records with satellite images to investigate channel change and bar evolution: a case study of the Padma River, Bangladesh. Environmental Earth Sciences, 77(3), 1–14.

Pal, R., & Pani, P. (2019). Remote sensing and GIS-based analysis of evolving planform morphology of the middle-lower part of the Ganga River, India. The Egyptian Journal of Remote Sensing and Space Science, 22(1), 1–10.

Petts, G. E. (1989). Historical analysis of fluvial hydrosystems. In G. E. Petts, H. Muller, & A. L. Roux (Eds.), Historical Change of Large Alluvial Rivers: Western Europe (pp. 1–18). Wiley.

Phillips, J. D. (2009). Avulsion regimes in southeast Texas rivers. Earth Surface Processes and Landforms, 34, 75–87.

ISSN:1624-1940
DOI 10.6084/m9.figshare.2632574
http://magellanes.com/

Rashid, H. E. (1991). Geography of Bangladesh (2nd ed.). The University Press Limited.

Rashid, M. B. (2020). Channel bar development and bankline migration of the Lower Padma River of Bangladesh. Arabian Journal of Geosciences, 13(14), 1–16.

Rashid, M. B., Habib, M. A., Khan, R., & Islam, A. R. M. T. (2021). Land transform and its consequences due to the route change of the Brahmaputra River in Bangladesh. International Journal of River Basin Management, 1–38.

Richard, G. A., Julien, P. Y., & Baird, D. C. (2005). Case study: modelling the lateral mobility of the Rio Grande below Cochiti Dam, New Mexico. Journal of Hydraulic Engineering, 131(11), 931–941.

Robert, A. (2014). River processes: an introduction to fluvial dynamics. Routledge.

Sarma, J. N., Bora, D., & Goswami, U. (2007). Change of river channel and bank erosion of the Burhi Dihing river (Assam), assessed using remote sensing data and GIS. Journal of the Indian Society of Remote Sensing, 35, 93–100.

Srivastava, P., Shukla, U. K., Mishra, P., Sharma, M., Sharma, S., Singh, I. B., et al. (2000). Luminescence chronology and facies development of Bhur sands in the interfluve region of central Ganga Plain, India. Current Science, 78, 498–503.

Sinha, R., & Ghosh, S. (2012). Understanding dynamics of large rivers aided by satellite remote sensing: a case study from Lower Ganga plains, India. Geocarto International, 27(3), 207–219.

Sinha, R., Jain, V., Babu, G. P., & Ghosh, S. (2005). Geomorphic characterization and diversity of the fluvial systems of the Gangetic Plains. Geomorphology, 70(3-4), 207-225.

Surian, N. (1999). Channel changes due to river regulation: the case of The Piave River, Italy. Earth Surface Processes and Landforms, 24, 1135-1151.

Thakur, P. K., Laha, C., & Aggarwal, S. P. (2012). River bank erosion hazard study of river Ganga, upstream of Farakka barrage using remote sensing and GIS. Natural Hazards, 61(3), 967–987.

Thoma, P. D., Gupta, C. S., & Bauer, E. M. (2001). Quantifying river bank erosion with scanning laser altimetry. International Archives of the Photogrammetry, Remote Sensing, Annapolis, 34(3/W4), 169–174.

Trimble, S. W., & Cooke, R. U. (1991). Historical sources for geomorphological research in the United States. The Professional Geographer, 43, 212–228.

Twidale, C. R. (1964). Erosion of an alluvial bank at Birdwood, South Australia. Zeitschrift für Geomorphologie, 8, 189–211.

Vörösmarty, C. J., Meybeck, M., Fekete, B., Sharma, K., Green, P., & Syvitski, J. P. M. (2003). Anthropogenic sediment retention: Major global impact from registered river impoundments.

ISSN:1624-1940
DOI 10.6084/m9.figshare.2632574
http://magellanes.com/

Global and Planetary Change, 39, 169–190.

Williams, G. P., & Wolman, M. G. (1984). Downstream effects of dams on alluvial rivers (Professional Paper 1286). U.S. Geological Survey.

Winterbottom, S. J. (2000). Medium and short-term channel planform changes on the River Tay and Tummel, Scotland. Geomorphology, 34, 195–208.

Wishart, D., Warburton, J., & Bracken, L. (2008). Gravel extraction and planform change in a wandering gravel-bed river: The River Wear, Northern England. Geomorphology, 94(1–2), 131-152.

Wolman, M. G. (1959). Factors influencing erosion of a cohesive river bank. American Journal of Science, 257, 204–216.

Yang, C., Cai, X., Wang, X., Yan, R., Zhang, T., Zhang, Q., & Lu, X. (2015). Remotely sensed trajectory analysis of channel migration in Lower Jingjiang Reach during the period of 1983–2013. Remote Sensing, 7(12), 16241-16256.

Yang, S. L., Milliman, J. D., Deng, B., Zhang, X. Y., & Luo, X. X. (2014). Downstream sedimentary and geomorphic impacts of the Three Gorges Dam on the Yangtze River. Earth Science Reviews, 138, 469-486.

Yao, Z., Ta, W., Jia, X., & Xiao, J. (2011). Right bank erosion and accretion along the Ningxia-Inner Mongolia reaches of the Yellow river from 1958 to 2008. Geomorphology, 127, 99–106.

Zawiejska, J., & Wyżga, B. (2010). Twentieth-century channel change on the Dunajec River, southern Poland: Patterns, causes and controls. Geomorphology, 117, 234–246.